

Article

## Electrochemical Aptasensor for Endocrine Disrupting 17 $\beta$ -Estradiol Based on a Poly(3,4-ethylenedioxythiophene)-Gold Nanocomposite Platform

Rasaq A. Olowu, Omotayo Arotiba, Stephen N. Mailu, Tesfaye T. Waryo, Priscilla Baker \* and Emmanuel Iwuoha

Sensor Lab, Department of Chemistry, University of the Western Cape, Bellville, 7535, South Africa; E-Mails: rolowu@uwc.ac.za (R.A.O.); oarotiba@uwc.ac.za (O.A.); 2970836@uwc.ac.za (S.N.M.); twaryo@uwc.ac.za (T.T.W.); eiwuoha@uwc.ac.za (E.I.)

\* Author to whom correspondence should be addressed; E-Mail: pbaker@uwc.ac.za; Tel.: +27-21-959-3051; Fax: +27-21-959-3055.

Received: 3 August 2010; in revised form: 17 September 2010 / Accepted: 11 October 2010 /

Published: 3 November 2010

---

**Abstract:** A simple and highly sensitive electrochemical DNA aptasensor with high affinity for endocrine disrupting 17 $\beta$ -estradiol, was developed. Poly(3,4-ethylenedioxythiophene) (PEDOT) doped with gold nanoparticles (AuNPs) was electrochemically synthesized and employed for the immobilization of biotinylated aptamer towards the detection of the target. The diffusion coefficient of the nanocomposite was  $6.50 \times 10^{-7} \text{ cm}^2 \text{ s}^{-1}$ , which showed that the nanocomposite was highly conducting. Electrochemical impedance investigation also revealed the catalytic properties of the nanocomposite with an exchange current value of  $2.16 \times 10^{-4} \text{ A}$ , compared to  $2.14 \times 10^{-5} \text{ A}$  obtained for the bare electrode. Streptavidin was covalently attached to the platform using carbodiimide chemistry and the aptamer immobilized via streptavidin—biotin interaction. The electrochemical signal generated from the aptamer—target molecule interaction was monitored electrochemically using cyclic voltammetry and square wave voltammetry in the presence of  $[\text{Fe}(\text{CN})_6]^{-3/-4}$  as a redox probe. The signal observed shows a current decrease due to interference of the bound 17 $\beta$ -estradiol. The current drop was proportional to the concentration of 17 $\beta$ -estradiol. The PEDOT/AuNP platform exhibited high electroactivity, with increased peak current. The platform was found suitable for the immobilization of the DNA aptamer. The aptasensor was able to distinguish 17 $\beta$ -estradiol from structurally similar endocrine

disrupting chemicals denoting its specificity to 17 $\beta$ -estradiol. The detectable concentration range of the 17 $\beta$ -estradiol was 0.1 nM–100 nM, with a detection limit of 0.02 nM.

**Keywords:** poly(3,4-ethylenedioxythiophene) (PEDOT); aptamer; modified electrode; avidin/biotin; square wave voltammetry

---

## 1. Introduction

Within the last ten years, many research articles describing modified electrodes using nanoparticles and conducting polymers have been published [1-4]. The field of electrochemical biosensors has grown rapidly because they provide fast, simple and inexpensive detection capabilities for biological binding events [5]. Conducting polymers can be obtained either chemically or electrochemically from their corresponding monomers, but the electropolymerization technique is more versatile. The film thickness and characteristics can be controlled by monitoring the polymerization charge during electropolymerization [6]. Conducting polymers exhibit unique properties such as catalysis, conductivity, biocompatibility, as well as their ability to act as an electrical plug connecting the bio recognition element to the surface of the electrode [7-9].

In order to improve sensitivity, selectivity and stability of biosensors different kinds of nanocomposite materials with enhanced performance have been developed and utilized for biosensor fabrication [10-12]. Nanocomposites containing inorganic nanoparticle and conducting polymers show a facile flow of electronic charge and unique properties that are obtained with these materials [2,13]. Nanocomposite materials exhibit exceptional electrical properties and optical properties compared to conducting polymer or metal nanoparticles used individually [13,14]. The electrocatalytic properties of nanoparticles are enhanced by the favorable environment supplied by the polymeric matrix [15]. The composite of conducting polymer-metal nanoparticle can be obtained from different metals and  $\pi$ -conjugated polymers as well as oligomer linkers which have received considerable attention due to the possibilities of creating suitable materials for electrocatalysis, chemical sensor and microelectronics [14,15]. Nanocomposite materials involving a hybrid of gold nanoparticle and carbon nanotube have been utilized for the construction of DNA biosensors [16]. Feng and his co-workers reported the use of a nanocomposite material consisting of gold nanoparticle and polyaniline nanotube membrane for DNA biosensor which was employed as a platform for immobilization of the DNA probe [2].

Among the various conducting polymers and conducting polymer nanocomposite materials developed and studied over the past ten years, poly(3,4-ethylenedioxythiophene) (PEDOT)-metal nanocomposites have been the focus of several studies as a result of its unique properties such as excellent stability against biological reducing agent due to their more ordered structure, high conductivity, high transparency and good thermal stability [17-19]. These unique properties make PEDOT an excellent material for various applications such as electrochromics, sensor light-emitting diodes and antistatic coatings [20,21]. The superior electrochemical stability of PEDOT may be attributed to the presence of the ethylenedioxy binding group on the  $\alpha$  and  $\beta$  position of thiophene ring in EDOT, which blocks coupling along the backbone, making the resulting polymer regiochemically

defined [21]. PEDOT has been reported to be excellent for synthesis of nanostructured materials and devices as a result of their electrical, electronic, magnetic, and optical properties which is similar to metals or semiconductors [22,23]. PEDOT coatings can be prepared by electrochemical polymerization in aqueous solution which allows the direct incorporation of water soluble anions [7,24]. Xiao and co-workers have developed an adenosine 5'-triphosphate (ATP) doped PEDOT for neural recording [25]. A silver nanograin incorporating a poly(3,4-ethylenedioxythiophene) (PEDOT) modified electrode for electrocatalytic sensing of hydrogen peroxide by simple electrochemical method was reported recently by Balamurugan and his co-workers [26].

One of the major classes of environmental contaminants are the endocrine disrupting chemicals (EDCs), which interfere with the function of the endocrine system. In recent years, these endocrine disrupting chemicals have become one of the main topics of research in the field of environmental sciences [27]. EDCs are defined as exogenous substances that cause adverse effect in organisms or its progeny, consequent to changes in endocrine function. They are ubiquitous in the environment because of their large number of uses in the residential, industrial and agricultural application [28]. The detection of these chemicals within the natural system is therefore necessary for protecting public and environmental health. Instrumental analysis methods such as high performance liquid chromatography (HPLC) and gas chromatography coupled with mass spectrophotometer (GC/MS) are very sensitive at detecting these toxic endocrine disrupting chemicals but are also very complicated to perform and require long analysis times to be accomplished. Using GC/MS an estimated concentration of 0.18–19.1 µg/kg was obtained in different foodstuffs in Germany compared to a calculated daily intake of 7.5 µg/day for nonylphenol, an endocrine disrupting chemical [29]. Concentrations of between 7.7–11,300 ng/L for some phenolic endocrine disrupting chemicals were obtained from river water in China using GC/MS coupled with the negative chemical ionization (NCI) technique [30]. The estimated daily human intake of estrogenic and anti-estrogenic counterparts, based on *in vitro* potencies relative to 17β-estradiol, has indicated that a woman taking birth control pills ingests about 6,675 µg/equivalent per day, postmenopausal estrogen treatment amount to 3,350 µg and ingestion of estrogen flavonoids in food represent 102 µg, while the daily ingestion of environmental organochlorine estrogen was estimated to be  $2.5 \times 10^{-6}$  µg [31].

Since the mid 1990s, a variety of adverse effects of endocrine disrupting chemicals on the endocrine systems of man and animals have been observed, which are of particular environmental concern [32]. Most EDCs are synthetic organic chemical that are introduced to the environment by anthropogenic sources but they can also be naturally generated by the estrogenic hormones 17β-estradiol and estrone [28]. It has been stated that the increasing incidence of breast and testicular cancers in humans may be caused by exposure to EDCs especially via drinking water whose source are often from surface waters [33,34]. The fate and behavior of EDCs are influenced by the structure and physicochemical parameters [35]. Most of these chemicals are present at low concentrations but many of them raised considerable toxicological concern. Children born to women exposed to high levels of polychlorobiphenyl (PCB) via consumption of polluted fish oil or rice oil have been reported to show delayed mental growth with lower Intelligence Quotient (IQ) scores, cognitive dysfunction, poorer visual identification memory and behavioral difficulties [36]. The incident of testicular cancer in men has increased significantly during the last decade. The incident of cancer in men under 50 years of age has increased approximately to 2–4% per annum since the 1960s in Great Britain, while in Denmark

the most common malignancy among men from age 25–34 years is testicular cancer. Breast cancer is the most common tumor in women in the World. The relative rate of recurrence varies five-fold between countries with the highest incidence in Western Europe and in North America. There has been a steady increase of breast cancer incidence rates over the last decades everywhere in Europe. The increased risk in of cancer has been linked to exposure to estrogenic chemicals and it has been reported that woman exposed to organochlorine chemicals such as DDT and certain PCB congeners may have higher incidence of breast cancer than non-exposed woman [36]. Prostate cancer is the second leading form of cancer in males in USA. Deaths due to prostate cancer have increased by 17% over the past three decades, despite improved diagnosis [36]. Considering the serious adverse effect of EDCs on human health and environment even at low concentration, it is urgent to identify an efficient method of estimating the concentration level of these chemicals in the environment.

To assess the impact of these chemical in the environment requires improved analytical methods and tools [37]. Recently more attention has been focused toward electrochemical aptasensor based on modified electrode for the determination of environmental pollutants. This is due to their excellent analytical performance such as specificity, selectivity, simplicity, wide linear range response, reproducibility and low cost [38,39].

In this work we report the electrochemical synthesis of poly(3,4-ethylenedioxythiophene)-PEDOT doped with gold nanoparticles (AuNPs) for the immobilization of biotinylated aptamer for the detection of 17 $\beta$ -estradiol—an endocrine disruptor. The single strand DNA which is the aptamer was chosen from that which has been reported in literature. This means that the sequence has been selected and patented and thus available for use. The sequence was designed according to literature [40]. The aptamer was biotinylated so as to effect a better immobilization chemistry using streptavidin—biotin interaction. The nanocomposite platform was characterized electrochemically by cyclic voltammetry in the presence of a [Fe (CN)<sub>6</sub>]<sup>-3/-4</sup> redox probe.

## 2. Experimental Section

### 2.1. Chemicals and Reagents

3,4-Ethylenedioxythiophene (EDOT), 3,3-dithiodipropionic acid (DPA), *N*-(3-dimethylaminopropyl)-*N*-ethylcarbodiimide hydrochloride (EDAC), *N*-hydroxysuccinimide (NHS), streptavidin, HAuCl<sub>4</sub> 3H<sub>2</sub>O, 17 $\beta$ -estradiol, sodium monohydrogen phosphate, potassium dihydrogen phosphate, lithium perchlorate, potassium ferricyanide [K<sub>3</sub>Fe(CN)<sub>6</sub>] and potassium ferricyanide [K<sub>4</sub>Fe(CN)<sub>6</sub>] and sodium dodecylsulphate were procured from Sigma-Aldrich (South Africa). All chemicals were of analytical grade and were used as received. Deionized water (18.2 M $\Omega$ ) purified by a milli-Q<sup>TM</sup> system (Millipore) was used throughout the experiment for aqueous solution preparation. A 76-mers biotinylated ssDNA aptamer synthesized by Inqaba Biotechnical Industries (Pty) Ltd., Hatfield, South Africa was used as aptamer probe. The sequence of the 76-mers sized biotinylated aptamer is given below:

**5'-BiotinGCTTCCAGCTTATTGAATTACACGCAGAGGGTAGCGGCTCTGCGC  
ATTCAATTGCTGCGCGCTGAAGCGCGGAAGC-3'**

## 2.2. Solutions

Phosphate buffer saline (PBS) of pH 7.5 containing 10 mM  $\text{Na}_2\text{HPO}_4$ ,  $\text{KH}_2\text{PO}_4$  and 0.1 M KCl was prepared, 5 mM (1:1) solution of  $\text{K}_3\text{Fe}(\text{CN})_6$  and  $\text{K}_4\text{Fe}(\text{CN})_6$  was prepared in 100 mL of PBS at pH 7.5. One hundred  $\mu\text{M}$  biotinylated DNA aptamer stock was prepared in tris EDTA (TE) buffer (pH 8.0) and stored at  $-20\text{ }^\circ\text{C}$ . Working DNA aptamer solution were prepared by diluting to the desired concentration in phosphate buffer storage at  $4\text{ }^\circ\text{C}$  and discarded after four weeks. Ten mL solution of 0.1 M lithium perchlorate containing 0.1 M EDOT monomer and 0.1 M of sodium dodecyl sulphate were prepared for the electropolymerization. A stock solution of 50 mL of binding buffer (pH 8.0) containing 100 mM tris HCl, 200 mM NaCl, 25 mM KCl, 10 mM  $\text{MgCl}_2$  and 5% ethanol were prepared. Stock solution of 1 mM *N*-[3-(dimethylaminopropyl)-*N*-3-ethylcarbodiimide hydrochloride] (EDAC), 1 mM *N*-hydroxysuccinimide (NHS), 1 mM 3,3-dithiodipropionic acid (DPA), as well as stock solution of 50  $\mu\text{g}/\text{mL}$  septravidin in PBS (pH 7.5) were prepared. One hundred  $\mu\text{M}$  stock solution of  $17\beta$ -estradiol (target) solution was prepared from which working target solution was prepared and diluted to desired concentrations with binding buffer. All stock solutions prepared were stored at  $4\text{ }^\circ\text{C}$  before and after use.

## 2.3. Electrochemical Measurement

A three electrode system was used to perform all electrochemical experiments. A gold electrode with a diameter of 1.6 mm was used as the working electrode, platinum wire as the counter electrode, and Ag/AgCl (3M  $\text{Cl}^-$ ) as the reference electrode. All electrochemical (voltammetric) experiments were recorded with Zahner IM6 electrochemical workstation (MeBtechnik).

Square wave voltammetry (SWV) measurements were recorded at amplitude 25 mV and frequency of 15 Hz with this electrochemical work station. Cyclic voltammetry measurements were recorded with the same electrochemical workstation. All solutions were de-aerated by purging with argon through it for 5 mins. The experiments were carried out under room temperature. UV/Vis spectra measurements were recorded with the Nicolette Evolution 100 Spectrometer (Thermo Electron Corporation, UK). Transmission electron microscopy (TEM) was performed in a Tecnai  $\text{G}^2\text{ F}_2\text{O}$  X-Twin MAT. TEM characterizations were performed by placing a drop of the solution on a carbon coated copper grid and dried under electric UV lamp for 30 minutes.

## 2.4. Preparation of Gold Nanoparticles

AuNP was prepared by citrate reduction of  $\text{HAuCl}_4$  solution according to literature [13,41]. The AuNP prepared was stored in a brown bottle at  $4\text{ }^\circ\text{C}$  before use.

## 2.5. Preparation of a Poly(3,4-ethylenedioxythiophene) Modified Gold Electrode

Prior to surface modification, the gold working electrode was polished to a mirror-like surface with alumina powder of sizes 1.0, 0.3 and 0.05  $\mu\text{m}$  respectively. The electrode was dipped in piranha solution for 10 minutes for effective cleaning and the electrode was then sonicated in ethanol and water consecutively for 5 mins. The electrode was further cleaned electrochemically in sulphuric acid by cycling between the potential of  $-200\text{ mV}$  to  $1,500\text{ mV}$  until a reproducible cyclic voltammogram

was obtained. Subsequently the gold electrode was rinsed with copious amount of water and absolute ethanol respectively. PEDOT film was deposited on the bare gold electrode from an aqueous solution of 0.1 M lithium perchlorate containing 0.1 M 3,4-ethylenedioxythiophene and 0.1 M sodium dodecyl sulphate by cycling the potential between  $-1,000$  mV to  $1,000$  mV at a scan rate of  $50$  mV/s for ten cycles, as shown in Figure 2.

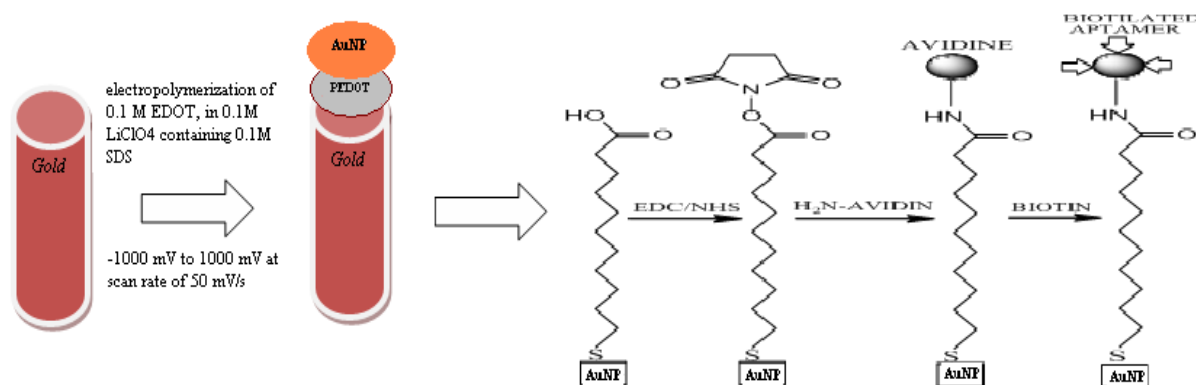
### 2.6. Fabrication of PEDOT—Gold Nanoparticle Modified Electrode

The PEDOT modified gold electrode prepared above was immersed in a colloidal gold nanoparticles solution for 24 h for self assembly of the gold nanoparticles on the PEDOT film to obtain a nanocomposite modified electrode.

### 2.7. Fabrication of the Aptasensor

A self assembled monolayer of 3,3'-dithiodipropionic acid (DPA) on the PEDOT/AuNP modified electrode was formed by incubation in an ethanolic solution of  $3$  mM dithiodipropionic acid for 45 min. The unbound DPA was removed by washing the electrode in absolute ethanol and then Millipore water respectively. After that the self assembled DPA was activated by immersing the electrode in the same volume of  $1$  mM each of EDAC and NHS to activate the carboxylic group for easy bonding with the amine group of streptavidin for 90 min. The electrode was then functionalized with streptavidin by incubating in PBS solution containing  $10$   $\mu\text{g/mL}$  streptavidin for 60 min at  $25$   $^{\circ}\text{C}$  and was later rinsed in PBS. The biotylated ssDNA aptamer was immobilized on the surface of the modified electrode via biotin-streptavidin interaction for 45 min at  $25$   $^{\circ}\text{C}$ . For the purpose of detection  $1$  nM aptamer was immobilized on the modified electrode surface. The PEDOT/AuNP/aptamer modified electrode was incubated with different concentration of  $17\text{-}\beta\text{-estradiol}$  prepared in binding buffer (Scheme 1).

**Scheme 1.** The schematic representation of the immobilization of aptamer on nanocomposite.



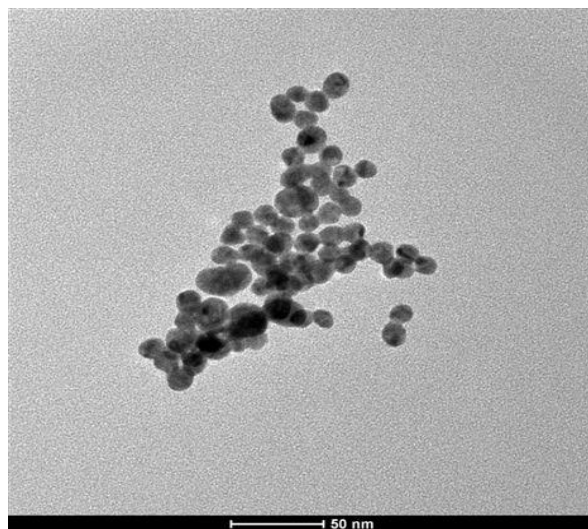
## 3. Results and Discussion

### 3.1. Characterization of Gold Nanoparticles

The formation of gold nanoparticles after reduction with citrate was confirmed by the use of UV-visible spectroscopy. A plasmon absorption band characteristic of gold nanoparticles was

observed at 525 nm [13,41]. The gold nanoparticles were further characterized with transmission emission microscopy (TEM) to determine the size of the nanoparticles. The nanoparticles have an average diameter of 18 nm. Figure 1 showed the TEM image of the synthesized gold nanoparticles.

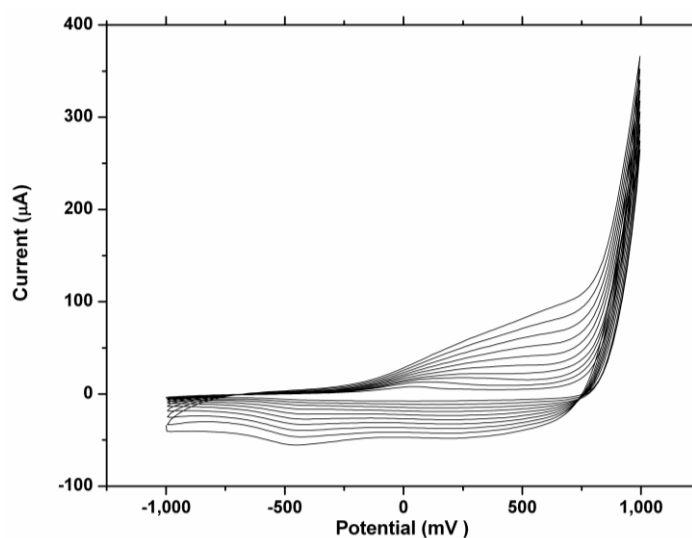
**Figure 1.** TEM image of gold nanoparticles.



### 3.2. Electrochemical Behavior of PEDOT Film Modified Gold Electrode

The PEDOT polymer film was obtained after ten successive cycles in 0.1 M lithium perchlorate containing 0.1 M of EDOT monomer and 0.1 M of sodium dodecyl sulphate (Figure 2).

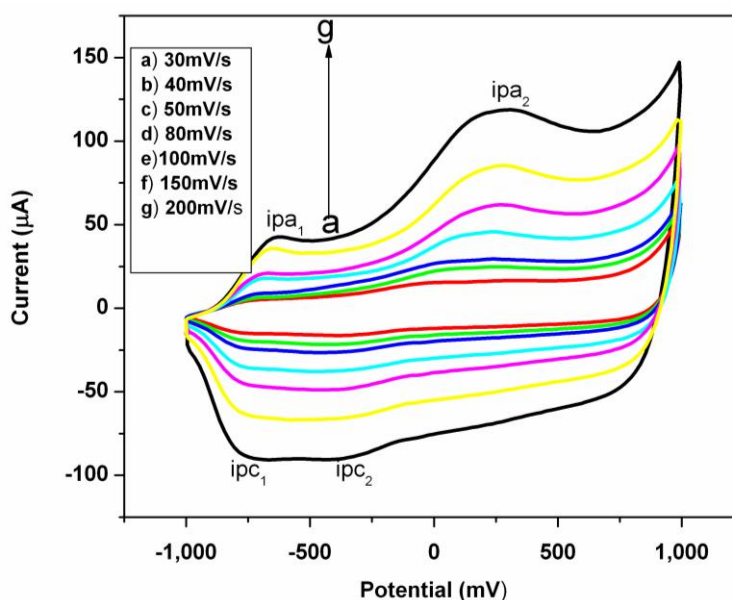
**Figure 2.** Electropolymerization of 0.1 M 3,4-ethylenedioxythiophene (EDOT) in 0.1 M lithium perchlorate containing 0.1 M sodium dodecyl sulphate.



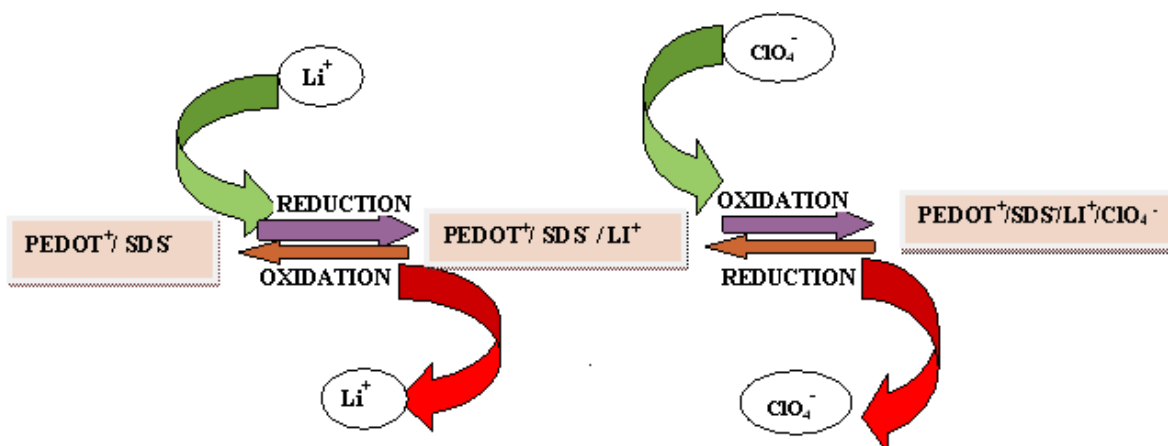
The electrochemical behavior of PEDOT film on a gold electrode resulting from polymerization of EDOT monomer was investigated in 0.1 M lithium perchlorate at different scan rates, by scanning from  $-1,000$  mV to  $1,000$  mV (Figure 3). PEDOT is electroactive based on the faradaic cathodic and anodic current observed in the CV. However the linear dependence of anodic peak ( $i_{pa}$ ) on the scan rate

shows that a thin film of surface bound conducting electroactive polymer with a surface confined redox chemistry was obtained [42]. Two sets of peaks were observed with the first redox couple ( $i_{pa1}$  and  $i_{pc1}$ ) situated at about  $-630$  mV while the second anodic peak ( $i_{pa2}$ ) was found at about  $+290$  mV. However, cathodic current peak intensity ( $i_{pc2}$ ) is not as clearly distinct as ( $i_{pa2}$ ) may be because it is located in the vicinity of ( $i_{pc1}$ ). It is assumed from the explanation that the existence of the two peak couples is an indication that the mechanism of the redox chemistry may involve both the cation and anion of the electrolytes diffusing in and out of the film. The electrochemical behavior of PEDOT was similar to that obtained in the literature.[43]. The redox chemistry is represented in Scheme 2. The film retained its electroactivity with no shift in the cathodic and anodic peak potential after thirty (30) cycles in 0.1 M lithium perchlorate. This suggest that the film is stable and not falling off the electrode [42,43].

**Figure 3.** Cyclic voltammograms of PEDOT film modified electrode in 0.1 M lithium perchlorate solution at different scan rates of (a) 30, (b) 40, (c) 50, (d) 80, (e) 100, (f) 150, (e) 200 mV/s.



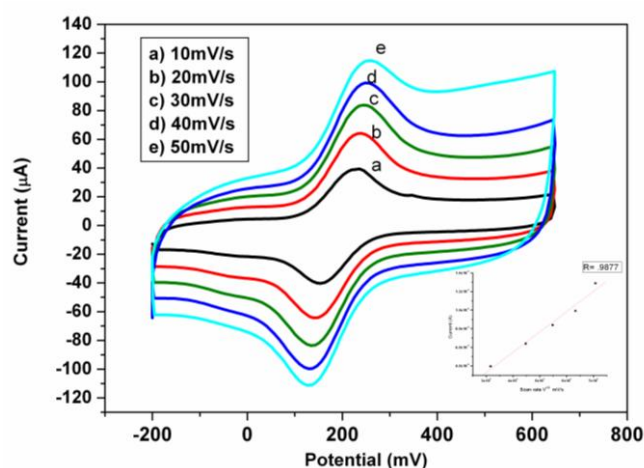
**Scheme 2.** Mechanism of the redox process.



### 3.3. Electrochemical Characteristics of the Nanocomposite

The electrochemical behavior of the nanocomposite was investigated using cyclic voltammetry. CV of the nanocomposite consisting of PEDOT and gold nanoparticles (Au/PEDOT/AuNPs) at different scan rates in  $[\text{Fe}(\text{CN})_6]^{-3/-4}$  as a redox probe, showed an increase in the peak current as the scan rate increases with no shift in the peak potential (Figure 4).

**Figure 4.** Cyclic voltammograms of the nanocomposite consisting of the conducting polymer PEDOT and gold nanoparticle in 5 mM  $[\text{K}_4\text{Fe}(\text{CN})_6]/[\text{K}_3\text{Fe}(\text{CN})_6]$  containing 0.1 M KCl at different scan rates showing electroactivity of the nanocomposite.



A linear dependence of anodic current on the scan rate was observed when a plot of  $i_{pa}$  versus scan rate was plotted with a correlation coefficient of 0.987. It can thus be deduced that the platform was characteristic of surface adsorbed species because  $I_{pa}$  versus scan rate was linear. There was no shift in potential and the  $i_{pa}/i_{pc}$  is unity also showing the stability of the PEDOT/AuNP platform in  $[\text{Fe}(\text{CN})_6]^{-3/-4}$ . The rate of electron transport ( $D_e$ ) was calculated to be  $6.50 \times 10^{-7} \text{ cm}^2 \text{ s}^{-1}$  using the Randle Sevcik equation:

$$I_p = 2.69 \times 10^5 n^{3/2} A D^{1/2} v^{1/2} C \quad (1)$$

where  $I_p$  = peak current,  $n$  = number of electron transfer,  $A$  = area of an electrode,  $D$  = diffusion coefficient,  $v$  = scan rate and  $C$  = concentration of bulk solution.

This value is high compared to the  $6.46 \times 10^{-8} \text{ cm}^2 \text{ s}^{-1}$  reported for PANI doped with polyvinyl sulphonate (PVS) and  $8.68 \times 10^{-9} \text{ cm}^2 \text{ s}^{-1}$  without doping [6]. The high value may be attributed to the doping of the PEDOT film with gold nanoparticles to produce a nanocomposite platform which further increased the conductivity of the PEDOT film resulting in a  $D_e$  value approximately one order of magnitude higher than reported for PANI doped with polyvinyl sulphonate (PVS) [6]. The chemistry involved between the PEDOT and Au nanoparticles is more than just physical adsorption. There is a chemical bonding between the well aligned sulphur of the PEDOT and AuNPs due to the affinity of sulphur for gold [44]. The reproducibility of the nanocomposite was investigated by cyclic voltammetry. The nanocomposite platform exhibited reversible electrochemistry in  $[\text{Fe}(\text{CN})_6]^{-3/-4}$  with a formal potential of  $223 \pm 6 \text{ mV}$  for six different measurements, demonstrating the good reproducibility of the nanocomposite.

### 3.4. Electrochemical Behavior of Modified Electrode Surface

Cyclic voltammograms at the bare gold electrode and the modified electrode in 5 mM  $[\text{Fe}(\text{CN})_6]^{-3/-4}$  are shown in Figure 5. A couple of well-defined redox peaks was observed at bare electrode with distinct cathodic peak ( $i_{pc}$ ) and the anodic peak current ( $i_{pa}$ ) values and a peak to peak separation  $\Delta E_p$  of 93 mV. The peak current at Au/PEDOT increased compared to bare electrode, which may be attributed to large surface area and good conductivity exhibited by the PEDOT. The PEDOT film act as a tiny conductive center which facilitate electron transfer which allow more of the  $[\text{Fe}(\text{CN})_6]^{-3/-4}$  to be accumulated on the surface of the PEDOT film modified electrode. Au/PEDOT/AuNP exhibited a couple of redox peaks with high peak current and a peak to peak separation  $\Delta E_p$  of 73 mV of shown in Table 1 which is an indication that the nanocomposite modified electrode possesses a larger effective surface area as well as good electrical conductivity [42].

**Figure 5.** Cyclic voltammograms of 5 mM  $[\text{K}_4\text{Fe}(\text{CN})_6]/[\text{K}_3\text{Fe}(\text{CN})_6]$  (1:1) containing 0.1 M KCl at (a) bare Au, (b) Au/PEDOT (c) Au/PEDOT/AuNP at a scan rate of 100 mV/s.

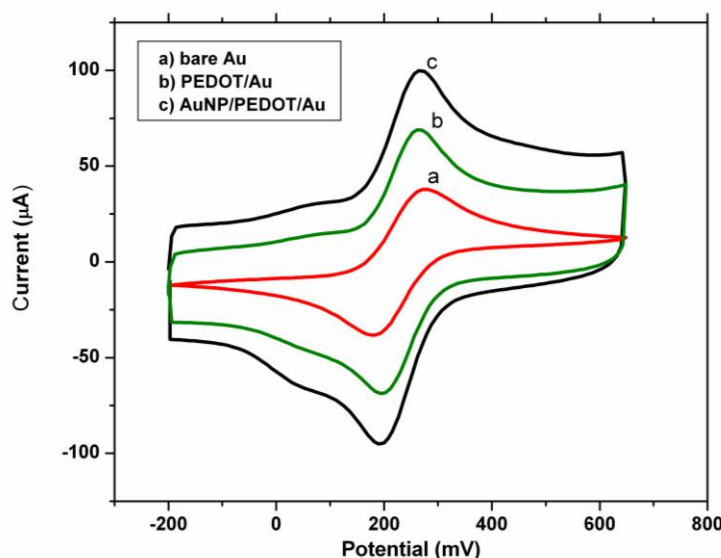


**Table 1.** The electrochemical parameter obtained for the modified surface during CVs.

	$E_{pa}$ mV	$E_{pc}$ mV	$i_{pc}$ (A)	$i_{pa}$ (A)	$\Delta E$	$i_{pa}/i_{pc}$
BAREGOLD (Au)	273	180	$3.788 \times 10^{-5}$	$3.693 \times 10^{-5}$	93	0.98
Au/PEDOT	267	191	$6.888 \times 10^{-5}$	$6.861 \times 10^{-5}$	76	0.99
Au/PEDOT/AuNP	270	197	$9.496 \times 10^{-5}$	$9.946 \times 10^{-5}$	73	1.05

### 3.5. Electrochemical Impedance Spectroscopy (EIS) of Au/PEDOT/AuNP

Electrochemical impedance spectroscopy (EIS) has been proven to be one of the most powerful tools for probing the features of surface-modified electrodes. EIS measurements were performed in the presence of 5 mM  $[\text{K}_4\text{Fe}(\text{CN})_6]/[\text{K}_3\text{Fe}(\text{CN})_6]$  (1:1) as a redox probe in 0.1 M phosphate buffer containing 0.1 M KCl at a potential of 234 mV and the frequency range is from 0.1 to  $10^5$  Hz; the

amplitude of the alternate voltage was 10 mV. The resistive and capacitive behavior of an electrode can be quantitatively evaluated by modeling an appropriate Randles equivalent circuit [45]. As shown in Figure 6(A) a Randles modified equivalent circuit was used to fit the impedance data. The parameters of the equivalent circuit included the solution resistance ( $R_s$ ), the Warburg impedance ( $Z_w$ ) resulting from the diffusion of the redox probe and charge transfer resistance ( $R_{ct}$ ).  $R_{ct}$  and CPE represent interfacial properties of the electrode which are highly sensitive to surface modification [46,47]. The double layer capacitance ( $C_{dl}$ ) is substituted with constant phase element (CPE) when taking into account the electrode roughness. The modification of the electrode with the nanocomposite changes the capacitance and the interfacial electron transfer resistance of the electrode. In the Nyquist diagram the semi circle observed at higher frequency, corresponds to the electron limited process whereas the linear part is the characteristics of the lower frequency range and represents the diffusion limited electron transfer process. The impedance response of the modified electrode in the presence of  $[\text{Fe}(\text{CN})_6]^{-3/-4}$  as a redox probe is depicted in Figure 6, while the bare electrode exhibited a very large semicircle at high frequency which represent the  $R_{ct}$  with a value of  $1.199 \times 10^3 \Omega$ . After the gold nanoparticles and PEDOT film were assembled on the gold electrode the  $R_{ct}$  decreased by an order of 1 to give a value of  $1.19 \times 10^2 \Omega$ . The decrease was found to be 90% compared to the bare electrode and is attributed to the presence of the AuNP and PEDOT film that plays an important role in accelerating the transfer of electrons, suggesting improved conductivity of the platform. Therefore the platform PEDOT/AuNP can be said to have catalytic effect on the rate of the charge transfer kinetic or the faradaic process of the redox probe. Exchange current was also used as a measure of the rate of electron transfer on the bare and the modified gold electrode. The  $i_0$  of electrode system is given by:

$$i_0 = \frac{RT}{nFR_{ct}} \quad (2)$$

where  $R$ ,  $F$  and  $n$  are gas constant, Faraday constant and number of electron transferred, respectively. The  $i_0$  values for the electron transferred reaction of  $[\text{Fe}(\text{CN})_6]^{-3/-4}$  on bare gold and Au/PEDOT/AuNP are  $2.14 \times 10^{-5}$  A and  $2.16 \times 10^{-4}$  A, respectively. From the calculated value it may be deduced that the rate of electron transfer was faster on the PEDOT/AuNP platform than the bare gold electrode. The catalytic effect of this platform may be attributed to enhanced surface and conductivity of the AuNP as well as an increase in the influx of the  $[\text{Fe}(\text{CN})_6]^{-3/-4}$  to the surface of the electrode as a result of the electrostatic attraction between cationic platform and the anionic  $[\text{Fe}(\text{CN})_6]^{-3/-4}$ . To further confirm the catalytic effect of this nanocomposite platform the estimation of the time constant and heterogeneous rate constant was done. The time constant value showed that the faradaic process of the  $[\text{Fe}(\text{CN})_6]^{-3/-4}$  probe is one order of magnitude faster on PEDOT/AuNP modified gold electrode than the bare gold electrode as shown in Table 2. In addition the increase in the heterogeneous rate constant at the nanocomposite modified electrode revealed a fast electron transfer of the redox probe due to the catalytic behavior of the nanocomposite platform. This result complemented the result obtained in Figure 4. The Nyquist plot for the nanocomposite is almost a straight line, which is a characteristic of diffusion controlled electrode process.

**Figure 6.** (A) Randles equivalent circuit and (B) Nyquist plots obtained for (a) bare Au, (b) Au/PEDOT/AuNP modified electrode. EIS measurements were carried out in 5 mM  $[\text{Fe}(\text{CN})_6]^{-3/-4}$  containing 0.1 M KCl.

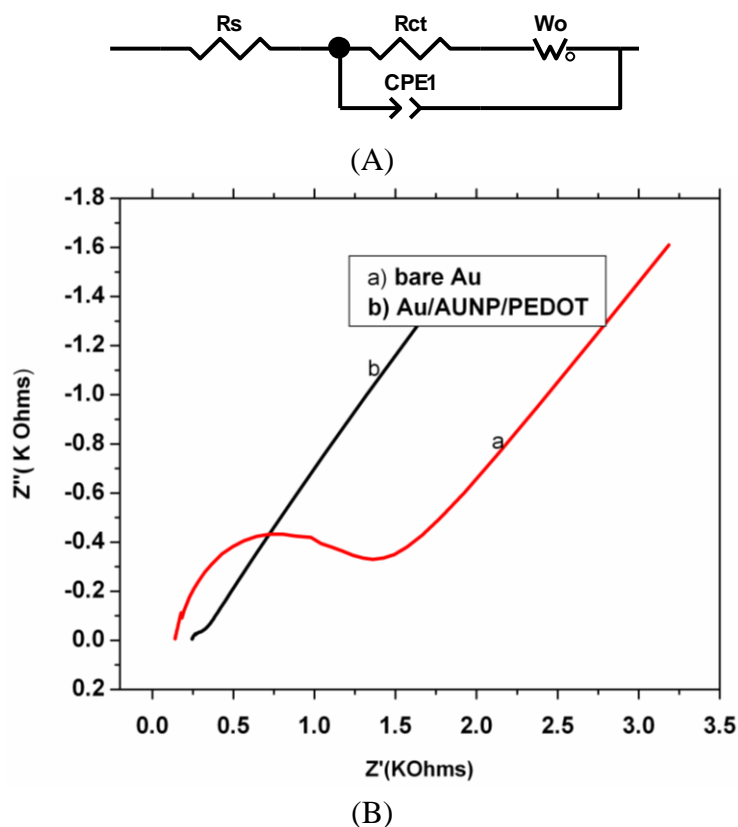


**Table 2.** Electrochemical impedance kinetic parameters of the bare electrode and the nanocomposite platform.

	Kinetic parameters		
	Exchange current	Time constant	Heterogeneous rate constant
Bare electrode	$2.14 \times 10^{-5}$ A	$1.49 \times 10^{-3}$ s/rad	$2.21 \times 10^{-3}$ cm/s
<b>PEDOT/AuNP platform</b>	$2.16 \times 10^{-4}$ A	$9.60 \times 10^{-5}$ s/rad	$2.23 \times 10^{-2}$ cm/s

The electrode coverage is a key factor which can be used to estimate the surface state of the electrode, and the charge resistance is related to it. The surface coverage ( $\theta$ ) of the nanocomposite on bare gold electrode can be estimated from EIS according to Equation (3) [48]:

$$\theta = 1 - \frac{R_{ct}^{\text{modified electrode}}}{R_{ct}^{\text{Bare electrode}}} \quad (3)$$

where  $R_{ct}$  denotes the charge transfer resistance. The surface coverage of ( $\theta$ ) of the electrode was estimated to be 90.1% which will enable more of the bioreceptor (aptamer) to be adsorbed on the surface of the electrode for better sensitivity of the aptasensor to its target.

### 3.6. Quantitative Analysis of 17 $\beta$ -Estradiol Using Aptamer Immobilized PEDOT/AuNP Modified Electrode

Electrochemical analysis was performed to confirm and optimize the condition for ssDNA aptamer immobilized on the surface of the modified electrode. Various concentrations of ssDNA aptamer (0.5  $\mu$ M–1.0  $\mu$ M) were initially mobilized on the modified electrode. The current changes in CV were measured before and after immobilization of ssDNA aptamer on the modified and current drop in CV was observed. The difference in current drop varies with the concentration of the ssDNA aptamer on the modified electrode which may be attributed to biotinylated ssDNA aptamer interference with the electron flow [49]. The decrease in current response with increase in concentration may be due to the electrostatic repulsion that exist between the negatively charge phosphate backbone of the DNA aptamer and the negatively charged hydroxyl ion substituent of the target in aqueous solution, which is one of the subtle substituents for aptamer discrimination within molecule of similar structures in the presence of  $[\text{Fe}(\text{CN})_6]^{-3/-4}$  as redox probe. Therefore binding of aptamer to charged small molecule in aqueous solution such as 17 $\beta$ -estradiol to aptamer can affect electron flow combined with diffusion rate in the presence of  $[\text{Fe}(\text{CN})_6]^{-3/-4}$  [48]. This also showed that PEDOT/AuNP could be a fine platform for immobilization of ssDNA aptamer.

The CV and SWV analysis was carried out against a series of 17 $\beta$ -estradiol concentrations (0.1 nM–100 nM) to probe the binding of the 17 $\beta$ -estradiol using 1 nM ssDNA aptamer immobilized on the surface of PEDOT/AuNP modified electrode. The interaction of the target-aptamer complex was monitored by reduction in the electron flux produced from redox reaction between ferrocyanide and ferricyanide. The current drop with increase in concentration was observed in SWV (Figure 7). The decrease in current after 17 $\beta$ -estradiol treatment was based on the specific interaction of aptamer and the target due to electrostatic repulsion that occur between the negatively charged phosphate backbone of the aptamer and negatively charge ion ( $\text{OH}^-$ ) of the target in solution. The formation of this aptamer-target complex changes the permeability of the layer toward charged ferricyanide ion and consequently the rate of their diffusion [49]. Although a wide range of 17 $\beta$ -estradiol was used, but the minimum concentration with which a current drop occurred was at 0.1 nM 17 $\beta$ -estradiol with slight change in potential and the increasing concentration dependence changes in current was seen till 100 nM in SWV.

The difference in peak potential ( $\Delta E = E_{\text{pa}} - E_{\text{pc}}$ ) from the cyclic voltammograms was increased which was dependent on the concentration of the target molecule. After the target molecule was adsorbed onto the surface of the biosensor, it exhibited a reduced peak current depending on the concentration. The decrease in peak current was observed which could be attributed to slow kinetics of the charge transfer, which is caused by the binding of 17 $\beta$ -estradiol to aptamer [40,49]. However with the series of 17 $\beta$ -estradiol dilutions tested it was found out that 0.1 nM 17 $\beta$ -estradiol was detectable with a lower concentration of 1 nM ssDNA aptamer immobilized on the nanocomposite platform. The high sensitivity of the aptasensor may be attributed to high surface coverage of 90.1% exhibited by the nanocomposite which significantly enhanced the loading of the DNA aptamer probe and hence markedly improve the sensitivity for the target as shown in Table 3 [16].

**Figure 7.** Square wave voltammograms of the electrochemical analysis of 17 $\beta$ -estradiol using 1 nM DNA aptamer immobilized on the nanocomposite platform showing current drop to concentration of target in range of 0.1–100 nM.

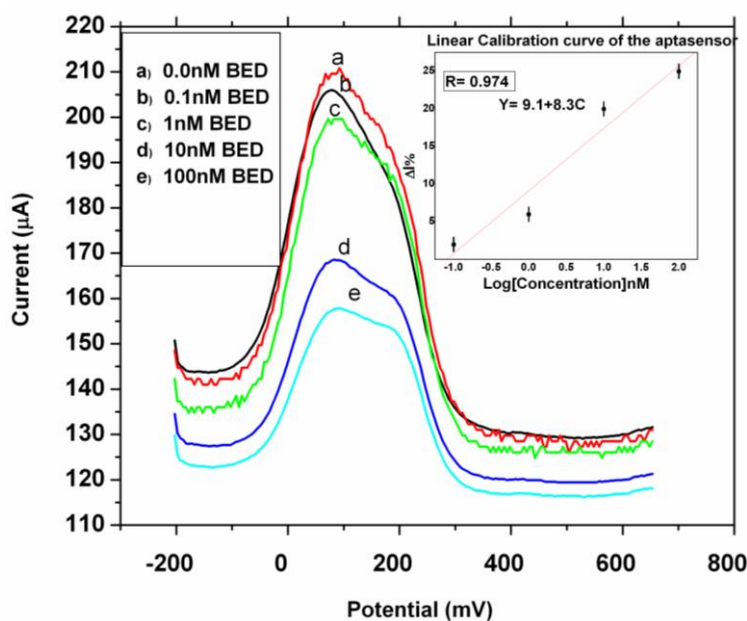


**Table 3.** Comparison of the aptasensor with other sensors.

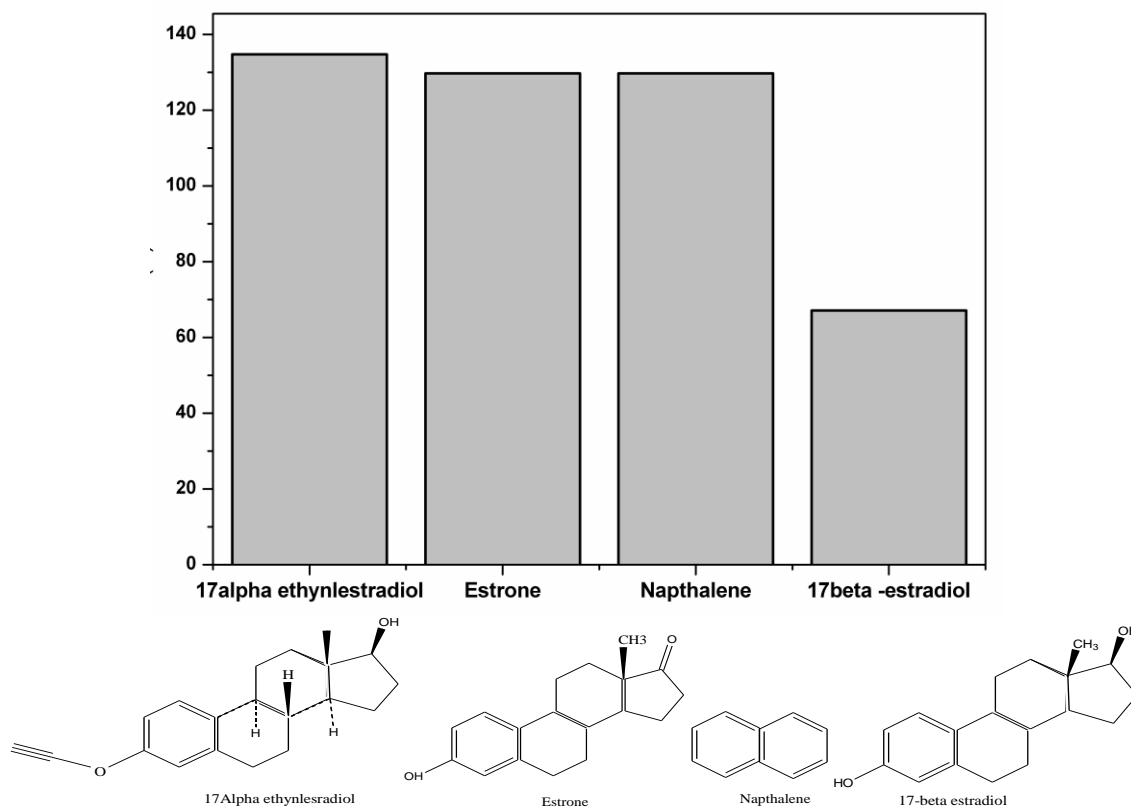
Methods	Linear range (M)	LOD(M)	Reference
Electrochemistry Au/PEDOT/AuNP	$0.1 \times 10^{-9}$ – $100 \times 10^{-9}$	$0.02 \times 10^{-9}$	This work
Electrochemistry Bare GCE	$4 \times 10^{-5}$ – $1 \times 10^{-3}$	$1 \times 10^{-5}$	[50]
Electrochemistry Poly-serine/GCE	$1 \times 10^{-7}$ – $3 \times 10^{-5}$	$2 \times 10^{-8}$	[51]
Electrochemistry GCE/nanoPt-MWNT	$5 \times 10^{-7}$ – $1.5 \times 10^{-5}$	$1.8 \times 10^{-7}$	[52]

### 3.7. Specificity and Selectivity Test of the Aptamer

Beside sensitivity, selectivity is also a remarkable feature for an aptamer sensor. Three different compounds that have similar structures as the target 17 $\beta$ -estradiol were taken as negative control and tested with the aptamer. A different signal must be differentiated from these substances compared to a 17 $\beta$ -estradiol aptamer [49]. Figure 8 compares the response of the fabricated aptasensor to 17 $\beta$ -estradiol and similarly structured substances in the presence of  $[\text{Fe}(\text{CN})_6]^{-3/-4}$  as probe. In Figure 8, 10 nM 17 $\alpha$ -ethynestradiol, estrone and naphthalene exhibited high current responses when incubated with aptasensor, which may be attributed to low binding action between the aptamer and the analogue chemicals. However, low current response was obtained when 17 $\beta$ -estradiol was incubated with aptasensor due to high binding action that existed between aptamer and 17 $\beta$ -estradiol resulting in the formation of an aptamer-target complex which hindered the electron flow as well as the diffusion rate in the presence of  $[\text{Fe}(\text{CN})_6]^{-3/-4}$ . The specificity of the target was mostly dependent on change in

position or absence of minor functional group such as H or OH in the molecules. This indicates that the designed electrode has a sufficient specificity for 17 $\beta$ -estradiol.

**Figure 8.** Current response of  $[\text{Fe}(\text{CN})_6]^{-3/-4}$  probe in the presence of DNA aptamer to 10 nM 17 $\alpha$ -ethynlestradiol, estrone, naphthalene and 17 $\beta$ -estradiol respectively.



### 3.8. Reproducibility and Stability.

The aptasensor is reproducible and stable. Square wave voltammetry repeatedly performed six times by incubating aptasensor with 10 nM 17 $\beta$ -estradiol gave a standard relative deviation of 5.2% ( $n = 6$ ) confirming the reproducibility of the sensing surface. The stability of the aptasensor was investigated by measuring the response of the aptasensor incubated with 10 nM 17 $\beta$ -estradiol after 15 days. It was found that there was almost 24.5% decrease in peak current response of the aptasensor thus the fabricated aptasensor retained 75.53% of its initial response after it was stored in the refrigerator at 4 °C for 15 days.

## 4. Conclusions

A nanocomposite platform on which a DNA aptamer was immobilized has been developed for the fabrication of an aptasensor employed for the detection of 17 $\beta$ -estradiol, an endocrine disruptor. The aptasensor was found to be sensitive at low concentrations due to the unique properties of the nanocomposite, which allow for the detection of the 17 $\beta$ -estradiol at concentrations as low as 0.02 nM. On the other hand, the result also demonstrated that the PEDOT/AuNP nanocomposite confined on the surface of the gold electrode can provide a promising platform for DNA aptamer construction.

## Acknowledgements

The research work was funded by the National Research Fund South Africa. We wish to thank the University of the Western Cape for the opportunity given to embark upon this research work.

## References

1. Stelian, L.; Ion, I.; Alina, C.I. Voltammetric Determination of Phenol at Platinum Electrodes Modified with Polypyrrole Doped with Ferricyanide. *Rev. Roum. Chim.* **2009**, *54*, 351-357.
2. Feng, Y.; Yang, T.; Zhang, W.; Jiang, C.; Jiao, K. Enhanced Sensitivity for Deoxyribonucleic Acid Electrochemical Impedance Sensor: Gold Nanoparticle/Polyaniline Nanotube Membranes. *Anal. Chim. Acta* **2008**, *616*, 144-151.
3. Xiaoxia, L.; Honglan, Q.; Lihua, S.; Qiang, G.; Chengxiao, Z. Electrochemical Aptasensor for the Determination of Cocaine Incorporating Gold Nanoparticles Modification. *Electroanalysis* **2008**, *20*, 1475-1482.
4. Aixue, L.; Yang, F.; Ma, Y.; Yang, X.R. Electrochemical Impedance Detection of DNA Hybridization Based on Dendrimer Modified Electrode. *Biosens. Bioelectron.* **2007**, *22*, 1716-1722.
5. Zhao, G.-C.; Yang, X. A Label-Free Electrochemical RNA Aptamer for Selective Detection of Theophylline. *Electrochem. Commun.* **2010**, *12*, 300-302.
6. Mathebe, N.G.R.; Morrin, A.; Iwuoha, E.I. Electrochemistry and Scanning Electron Microscopy of Polyaniline/Peroxidase-Based Biosensor. *Talanta* **2004**, *64*, 115-120.
7. Sakmeche, N.; Bazzaoui, E.A.; Fall, M.; Aeiyaeh, S.; Jouini, M.; Lacroix, J.C.; Aaron, J.J.; Lacaze, P.C. Application of Sodium Dodecyl Sulphate (SDS) Micellar Solution as an Organised Medium for Electropolymerization of Thiopene Derivatives in Water. *Synth. Meth.* **1997**, *84*, 191-192.
8. Ogura, K.; Nakaoka, K.; Nakayama, M. Studies on Ion Transport During Potential Cycling of a Prussian Blue (Inner) Polyaniline (Outer) Bilayer Electrode by Quartz Crystal Microbalance and Fourier Transform Infrared Reflection Spectroscopy. *J. Electroanal. Chem.* **2000**, *486*, 119-125.
9. Lupu, S.; Mihailiciuc, C.; Pigani, L.; Renato, S.; Nicolae, T.; Chiara, Z. Electrochemical Preparation and Characterization of Bilayer Film Composed by Prussian Blue and Conducting Polymer. *Electrochem. Commun.* **2002**, *4*, 750-758.
10. Xueliang, W.; Tao, Y.; Yuayua, F.; Kui, J.; Guiaun, L. A Novel Hydrogen Peroxide Biosensor Based on the Synergic Effect of Gold-Platinum Alloy Nanoparticle/Polyaniline Nanotube/Chitosan Nanocomposite Membrane. *Electroanalysis* **2009**, *21*, 819-825.
11. Yang, T.; Zhang, W.; Du, M.; Jiao, K. A PDDA/Poly(2,6-pyridinedicarboxylic acid)-CNTs Composite Film DNA Electrochemical Sensor and its Application for the Detection of Specific Sequences Related to PAT Gene and NOS Gene. *Talanta* **2008**, *75*, 987-994.
12. Jiang, C.; Yang, T.; Jiao, K.; Gao, H. A DNA Electrochemical Sensor with Poly-L-Lysine/Single-Walled Carbon Nanotubes Films and its Application for the Highly Sensitive EIS Detection of PAT Gene Fragment and PCR Amplification of NOS Gene. *Electrochim. Acta* **2008**, *53*, 2917-2924.

13. Hussain, I.; Brust, M.; Papworth, A.J.; Cooper, A.I. Preparation of Acrylate-Stabilized Gold and Silver Hydrosols and Gold-Polymer Composite Films. *Langmuir* **2003**, *19*, 4831-4835.
14. Liu, F.-J.; Huang, L.-M.; Wen, T.-C.; Li, C.-F.; Huang, S.-L.; Gopalan, A. Platinum Particles Dispersed Polyaniline-Modified Electrodes Containing Sulfonated Polyelectrolyte for Methanol Oxidation. *Synth. Meth.* **2008**, *158*, 767-774.
15. O'Mullane, A.P.; Dale, S.E.; Macpherson, J.V.; Unwin, P.R. Fabrication and Electrocatalytic Properties of Polyaniline/Pt Nanoparticle Composite. *Chem. Commun.* **2004**, *14*, 1606-1607.
16. Zhou, N.; Yang, T.; Jiang, C.; Du, M.; Jiao, K. Highly Sensitive Electrochemical Impedance Spectroscopic Detection of DNA Hybridization Based on Aunano-CNT/Pannano Films. *Talanta* **2009**, *77*, 1021-1026.
17. Alemán, C.; Teixeira-Dias, B.; Zanuy, D.; Estrany, F.; Armelin, E.; del Valle, L.J. A Comprehensive Study of the Interactions between DNA and Poly(3,4-ethylenedioxythiophene). *Polymer* **2009**, *50*, 1965-1974.
18. Argun, A.A.; Cirpan, A.; Reynolds, J.R. Using Poly(3,4-ethylenedioxythiophene) Polystyrene Sulfonate (PEDO/PSS). *Adv. Mater.* **2003**, *15*, 1338-1341.
19. Drillet, J.F.; Dittmeyer, R.; Juttner, K. Study of the Activity and Longterm Stability of PEDOT at Platinum Catalyst Support for the DMFC Anode. *J. Appl. Electrochem.* **2007**, *37*, 1219-1226.
20. Dong-Hun, H.; Jae-Woo, K.; Su-Moon, P. Electrochemistry of Conducting Polymer 38. Electrodeposited Poly(3,4-ethylenedioxythiophene) Studied by Current Sensing Atomic Force Microscopy. *J. Phys. Chem. B* **2006**, *110*, 14874-14880.
21. Jui, H.C.; Chi-An, D.; Wen-Yen, C. Synthesis of Highly Conductive EDOT Copolymer Film via Oxidative Chemical *in situ* Polymerization. *J. Polym. Sci. A* **2008**, *46*, 1662-1673.
22. Zotti, G.; Vercelli, B.; Berlin, A. Gold Nanoparticle Linking to Polypyrrole and Polythiophene Monolayers and Multilayers. *Chem. Mater.* **2008**, *20*, 6509-6516.
23. Prakash, A.; Ouyang, J.; Lin, J.L.; Yan, Y. Polymer Memory Device Based on Conjugated Polymer and Gold Nanoparticles. *J. Appl. Phys.* **2006**, *100*, 054309:1-054309:5.
24. Pigani, L.; Heras, A.; Colina, Á.; Seeber, R.; López-Palacios, J. Electropolymerisation of 3,4-ethylenedioxythiophene in Aqueous Solutions. *Electrochem. Commun.* **2004**, *6*, 1192-1198.
25. Xiao, Y.H.; Li, C.M.; Toh, M.L.; Xue, R. Adenosine 5' Triphosphate Incorporated Poly(3,4-ethylenedioxythiophene) Modified Electrode a Bioactive Platform with Electroactivity, Stability and Biocompatibility. *Chem. Biol. Interact.* **2005**, *157-158*, 423-426.
26. Balamurugan, A.; Chen, S. Silver Nanograin Incorporated PEDOT Modified Electrode for Electrocatalytic Sensing of Hydrogen Peroxide. *Electroanalysis* **2009**, *12*, 1419-1423.
27. Zhang, Y.; Zhou, J.L. Occurrence and Removal of Endocrine Disrupting Chemicals in Wastewater. *Chemosphere* **2008**, *73*, 848-853.
28. Schilirò, T.; Pignata, C.; Rovere, R.; Fea, E.; Gilli, G. The Endocrine Disrupting Activity of Surface Waters and of Wastewater Treatment Plant Effluents in Relation to Chlorination. *Chemosphere* **2009**, *75*, 335-340.
29. Klaus, G.; Volkmar, H.; Bjoern, T.; Einhard, K.; Hartmut, P.; Torsen, R. Endocrine Disrupting Nonylphenols Are Ubiquitous in Food. *Envir. Sci. Technol.* **2002**, *36*, 1676-1680.

30. Zhao, J.L.; Ying, G.G.; Wang, L.; Yang, J.F.; Yang, X.B.; Yang, L.H.; Li, X. Determination of Phenolic Endocrine Disrupting Chemicals and Acidic Pharmaceuticals in Surface Water of the Pearl Rivers in South China by Gas Chromatography-Negative Chemical Ionization-Mass Spectrometry. *Sci. Total Envir.* **2009**, *407*, 962-974.
31. Safe, S. Endocrine Disruptors and Human Health: Is There a Problem. *Toxicology* **2004**, *205*, 3-10.
32. Pothitou, P.; Voutsas, D. Endocrine Disrupting Compounds in Municipal and Industrial Wastewater Treatment Plants in Northern Greece. *Chemosphere* **2008**, *73*, 1716-1723.
33. Safe, S. Clinical Correlate of Environmental Endocrine Disruptors. *Trend Endocrine Mat.* **2005**, *16*, 139-144.
34. Synder, S.A.; Westerhoff, P.; Yoon, Y. Pharmaceutical, Personal Care Product and Endocrine Disrupting Chemical in Water Implication for Water Industry. *Environ. Eng. Sci.* **2003**, *20*, 449-469.
35. Jiang, J.Q.; Yin, Q.; Zhou, J.L.; Pearce, P. Occurrence and Treatment Trials of Endocrine Disrupting Chemicals (Edcs) in Wastewaters. *Chemosphere* **2005**, *61*, 544-550.
36. Amaral Mendes, J.J. Endocrine Disrupters a Major Medical Challenge. *Food Chem. Toxicol.* **2002**, *40*, 781-788.
37. Koester, C.J.; Simoni, S.C.; Esser, B.K. Environmental Analysis. *Anal. Chem.* **2003**, *75*, 2813-2821.
38. Cheng, A.K.H.; Sen, D.; Yu, H.Z. Design and Testing of Aptamer-Based Electrochemical Biosensors for Proteins and Small Molecules. *Bioelectrochemistry* **2009**, *77*, 1-12.
39. Li, X.; Shen, L.; Zhang, D.; Qi, H.; Gao, Q.; Ma, F.; Zhang, C. Electrochemical Impedance Spectroscopy for Study of Aptamer-Thrombin Interfacial Interactions. *Biosen. Bioelectron.* **2008**, *23*, 1624-1630.
40. Kim, Y.S.; Jung, H.S.; Matsuura, T.; Lee, H.Y.; Kawai, T.; Gu, M.B. Electrochemical Detection of 17 $\beta$ -estradiol Using DNA Aptamer Immobilized Gold Electrode Chip. *Biosens. Bioelectron.* **2007**, *22*, 2525-2531.
41. Robertson, D.; Tiersch, B.; Kosmella, S.; Koetz, J. Preparation of Crystalline Gold Nanoparticles at the Surface of Mixed Phosphatidylcholine-Ionic Surfactant Vesicles. *J. Colloid Interface Sci.* **2007**, *305*, 345-351.
42. Vasantha, V.S.; Thangamuthu, R.; Mingchen, S. Electrochemical Polymerization of Poly(3,4-ethylenedioxythiophene) from Aqueous Solution Containing Hydroxyl Propyl- $\beta$ -cyclodextrine and the Electrocatalytic Behavior of Modified Electrode towards Oxidation of Sulphur Oxoanion and Nitrite. *Electroanalysis* **2008**, *20*, 1754-1759.
43. Damlin, P.; Kvarnström, C.; Ivaska, A. Electrochemical Synthesis and *in situ* Spectroelectrochemical Characterization of Poly(3,4-ethylenedioxythiophene) (PEDOT) in Room Temperature Ionic Liquids. *J. Electroanal. Chem.* **2004**, *570*, 113-122.
44. Shin, H.C.; Su-Moon, P. Electrochemistry of Conductive Polymers 39. Contacts between Conducting Polymers and Noble Metal Nanoparticles Studied by Current-Sensing Atomic Force Microscopy. *J. Phys. Chem. B* **2006**, *110*, 25656-25664.
45. Abd-Elgawad, R.; Josep, S.; Lluís, A.; ;Baldrich, E.; Sullivan, C. Reusable Impedimetric Aptasensor. *Anal. Chem.* **2005**, *77*, 6320-6323.

46. Arotiba, O.A.; Joseph, O.; Everlyne, S.; Nicolette, H.; Tesfaye, W.; Nazeem, J.; Baker, P.G.L.; Iwuoha, E.I. An Electrochemical DNA Biosensor Developed on a Nanocomposite Platform of Gold and Poly(propyleneimine) Dendrimer. *Sensors* **2008**, *8*, 6791-6809.
47. Arotiba, O.A.; Owino, J.H.; Baker, P.G.; Iwuoha, E.I. Electrochemical Impedimetry of Electrodeposited Poly(propyleneimine) Dendrimer Monolayer. *J. Electroanal. Chem.* **2010**, *638*, 287-292.
48. Zhang, R.; Di-Jin, G.; Chen, D.; Hu, X. Simultaneous Electrochemical Determination of Dopamine, Ascorbic Acid, and Uric Acid Using (Acid Chrome Blue K) Modified Glassy Carbon Electrode. *Sens. Acuat. B* **2009**, *138*, 174-181.
49. Kim, Y.S.; Niazi, J.H.; Gu, M.B. Specific Detection of Oxytetracycline Using DNA Aptamer-Immobilized Interdigitated Array Electrode Chip. *Anal. Chim. Acta* **2009**, *634*, 250-254.
50. Salci, B.; Biryol, I. Voltammetric Investigation of  $\beta$ -estradiol. *Pharmaceut. Biomed. Anal.* **2002**, *28*, 753-758.
51. Song, J.C.; Yang, J.; Hu, X.M. Electrochemical Determination of Estradiol Using a Poly(L-Serine) Film-Modified Electrode. *J. Appl. Electrochem.* **2008**, *38*, 833-836.
52. Lin, X.Q.; Li, Y.X. A Sensitive Determination of Estrogens with a Pt Nano-Clusters/ Multi-Walled Carbon Nanotubes Modified Glassy Carbon Electrode. *Biosens. Bioelectron.* **2006**, *22*, 253-256.

© 2010 by the authors; licensee MDPI, Basel, Switzerland. This article is an open access article distributed under the terms and conditions of the Creative Commons Attribution license (<http://creativecommons.org/licenses/by/3.0/>).